Molecular and functional characterization of twelve new mutations out of seventeen in *CYBB* gene leading to different sub-types of X-linked chronic granulomatous disease

Michelle Mollin[1], Sylvain Beaumel[1], Cécile Martel[1], Bénédicte Vigne[1], Nathalie Roux-Buisson[2,3], John Rendu[2,3], Vincent Barlogis[4], Gaud Catho[5], Claire Dumeril[6], Fanny Fouyssac[7], Delphine Monnier[8], Virginie Gandemer[9], Matthieu Revest[10], Jean-Paul Brion[11], Cécile Bost-Bru[12], Eric Jiezorski[13], Laurence Eitenschenck[6], Clémence Jarrasse[6], Stéphanie Drillon-Haus[14], Marie Houachée-Chardin[5], Morgane Hancart[13], Gérard Michel[4], Yves Bertrand[5], Dominique Plantaz[12], Jadranka Kelecic[15], Rasa Traberg[16], Leena Kainulainen[17], Julien Fauré[2,3], Franck Fieschi[18], Marie José Stasia[1,18*]

[1]Centre Hospitalier Universitaire Grenoble Alpes, Pôle de Biologie, CGD Diagnosis and Research Centre (CDiReC), Grenoble, France

[2]Centre Hospitalier Universitaire Grenoble Alpes, Pôle de Biologie, Laboratoire de Biochimie et Génétique Moléculaire, Université Grenoble Alpes, Grenoble, France

[3]Grenoble Institut des Neurosciences, Inserm U1216-Eq. 4 C-MyPath, La Tronche, France

[4]Centre Hospitalier Universitaire La Timone, Service de Pédiatrie et Hématologie Pédiatrique, Marseille, France

[5] Hospices Civiles de Lyon, Institut d'Hématologie et d'Oncologie Pédiatrique, Lyon, France

[6]Centre Hospitalier Annecy Genevois, Servie de Pédiatrie, Pringy, France

[7]Centre Hospitalier Universitaire de Nancy, Département d'Onco-hématologie Pédiatrique, Vandoeuvre-lès-Nancy, France

[8]Centre Hospitalier Universitaire Pontchaillou, Laboratoire d'Immunologie cellulaire, Rennes, France

[9]Centre Hospitalier Universitaire de Rennes, Service d'Onco-hématologie Pédiatrique, Rennes, France

[10]Centre Hospitalier Universitaire de Rennes, Service des Maladies Infectieuses et Réanimation Médicale, Rennes, France

[11]Centre Hospitalier Universitaire Grenoble Alpes, Pôle Médecine Aigue et Communautaire, Service d'Infectiologie, Grenoble, France

[12]Centre Hospitalier Universitaire Grenoble Alpes, Département de Pédiatrie, Pôle Couple/Enfant, Grenoble, France

[13]Centre Hospitalier Universitaire de Montpellier, Service de Pédiatrie et Hématologie Pédiatrique, Montpellier, France

[14]Centre Hospitalier Universitaire de Strasbourg, Hôpital de Hautepierre, Service de Pédiatrie et Onco-hématologie, Strasbourg, France

[15]Klinicki Bolnicki Centar Zagreb, Zagreb, Croatia

[16]Hospital of Lithuanian University of Health Sciences Kauno klinikos, Kaunas, Lithuania

[17]University Hospital of Turku, Department of Pediatrics, Turku, Finland, University of Turku, Faculty of Medicine

[18]Univ. Grenoble Alpes, CEA, CNRS, IBS, F-38044 Grenoble, France, Grenoble, France

*Corresponding author: Marie Jose Stasia; marie-jose.stasia@univ-grenoble-alpes.fr; ORCID number 0000-0003-4466-4880

Abstract

Chronic Granulomatous Disease (CGD) is a rare inherited disorder in which phagocytes lack NADPH oxidase activity. The most common form is the X-linked CGD (X-CGD), caused by mutations in the *CYBB* gene. We fully investigated 16 male patients and their relatives suspected of suffering from X-CGD. They were classified as suffering from different variants of CGD ($X91^0$, $X91^-$ or $X91^+$), according to NOX2 expression and NADPH oxidase activity in neutrophils. Twelve mutations were novel (10 $X91^0$-CGD and 2 $X91^-$-CGD). Of the 13 $X91^0$-CGD mutations, 4 deletions, one insertion, one duplication and 6 point mutations (3 missense, 2 nonsense and one splice mutation) were found. Surprisingly, one $X91^0$-CGD was due to a new and rare double missense mutation Thr208Arg-Thr503Ile. We investigated the pathological impact of each single and double mutation, using stable transfection of each mutated cDNA in the NOX2 knock-out PLB-985 cell line. We also fully characterized the phenotype of an $X91^+$-CGD case due to the missense mutation Gly412Glu in the dehydrogenase domain of NOX2. The impact of new missense mutations is discussed in the context of a new 3 D model of the dehydrogenase domain of NOX2. Both mutations leading to $X91^-$-CGD were novel; one deletion -67delT was localized in the promoter region of *CYBB*, the second one c.253-1879A>G mutation activates a splicing donor site, which unveils a cryptic acceptor site, leading to the inclusion of a 124-nucleotide pseudo-exon between exons 3 and 4 and responsible for the partial loss of NOX2 expression. Both $X91^-$-CGD mutations were characterized by a low cytochrome b_{558} expression and faint NADPH oxidase activity. Our study demonstrates that low NADPH oxidase activity found in both $X91^-$-CGD patients correlates with mild clinical forms of CGD.

Keywords

Introduction

Chronic granulomatous disease (CGD) is a rare genetic disorder belonging to innate immunodeficiency syndromes. CGD is due to a defect in the NADPH oxidase complex of phagocytes, highly expressed in phagocytic cells like neutrophils, monocytes and macrophages. The pathophysiological consequence is a defect in reactive oxygen species (ROS) production normally responsible for the killing of bacteria and fungi during an infection. Thus, CGD is generally diagnosed early, before the age of 2 by recurrent and severe infections, although some rare cases may remain undiagnosed until later childhood or even adult life ({Roos, 2016 #280}). The incidence of CGD is about 1 in 250,000 newborn individuals. CGD is a genetically heterogeneous disease with all ethnic groups equally affected. The NADPH oxidase complex is composed of a membrane-bound flavocytochrome b_{558} (cytb_{558}), the redox center of the enzyme, consisting of an α subunit, p22^{phox}, and a β subunit, NOX2 (also named gp91^{phox}), and three cytosolic components: p47^{phox}, p67^{phox} and p40^{phox}. CGD is caused by mutations located in any of these five subunits. NOX2 is the flavin- and heme-containing oxidase element capable of transferring electrons from NADPH in the cytosol to molecular oxygen in the extracellular or intra-phagosomal compartment, while p22^{phox} stabilizes the expression of this component in phagocytic cells. In neutrophils, the defect in expression of one of these two subunits compromises the expression of the other ({Nauseef, 2019 #295}). NOX2 is the flavinoxidase element capable of transferring electrons, while p22^{phox} stabilizes the expression of this component in phagocytic cells. In neutrophils the defect of expression of one of these two sub-units compromises the expression of the other ({Yu, 1999 #2}). A small G protein, Rac2 is also involved in regulating NADPH oxidase activity and can be mutated in rare cases, leading to an innate immunodeficiency ({Gu, 2002 #301;Yu, 2001 #302;Roberts, 1999 #303; Sharapova, 2019 #304;Hsu, 2019 #305;Williams, 2000 #307;Ambruso, 2000 #308}). In resting cells, membrane and cytosolic components of the NADPH oxidase complex are dissociated, while in stimulated phagocytes they become associated at the membrane, leading to an active oxidase complex able to produce superoxide anions ({Sumimoto, 2008 #15}).

On the basis of the mode of inheritance, two forms of the CGD are known: an autosomal form (AR-CGD) with mutations in *CYBA* (OMIM number 233690), *NCF1* (OMIM number 233700), *NCF2* (OMIM number 233710) or *NCF4* (OMIM number 613960), encoding p22^{phox}, p47^{phox}, p67^{phox} and p40^{phox} proteins, respectively. In the X-linked form of CGD (X91-CGD), mutations are present in *CYBB* (OMIM number 306400) encoding NOX2, which accounts for more than 60% of all CGD cases ({Roos, 2010 #3;Roos, 2010 #86 ;van de Geer, 2018 #311}). Clear information on the severity of CGD according to the genetic forms is difficult to establish. In addition, the majority of mutations affecting the membrane cytb_{558} are associated with severe clinical features of CGD, when no measurable NADPH oxidase activity is found ({van den Berg, 2009 #4}). Indeed, X91-CGD patients with mutations in *CYBB* can be classified as having different variant forms (X91^0, X91$^-$ or X91$^+$), according to the level of cytb_{558} expression and NADPH oxidase activity in their phagocytes ({O'Neill, 2015 #326}). The *CYBB* gene, encoding NOX2, encompasses 13 exons spanning about 30 kb of the human X chromosome DNA [{Royer-Pokora, 1986 #344;Teahan, 1987 #347}]. X91^0-CGD, which represents more than 90% of X91-CGD cases, is characterized by an absence of cytb_{558} expression and NADPH oxidase activity and is related to the most severe clinical form. A few numbers of cases with "variant" forms of the disease, called X91$^-$-CGD have also been described, in which low levels of cytb_{558} expression are accompanied

by a proportionally decreased NADPH oxidase activity [{Beaumel, 2014 #337}]. Mutations associated with this phenotype are usually located in the coding region of *CYBB*. These variants are of interest because they cause a structural disorganization, leading either to an incomplete loss of protein or to a partial dysfunction, or both {Stasia, 2008 #6}. The severity of the clinical forms of these variants varies considerably, relating to the level of NADPH oxidase activity to the level of NADPH oxidase activity ({Kuhns, 2010 #316}). Very rare mutations (5 published cases) in the upstream promoter region of *CYBB*, leading to the X91$^-$-CGD phenotype have also been described [{Newburger, 1994 #349;Weening, 2000 #350 ;Stasia, 2003 #351;Defendi, 2009 #5}]. These mutations are located between the "CCAAT" and the "TATA" boxes in a consensus binding site for the ets family of transcription factors in the NOX2 promoter region, and are responsible for defects in *CYBB* transcription [{Voo, 1999 #352}]. A striking point is that in most of the X91$^-$-CGD cases characterized by a mutation in the *CYBB* promoter, the CGD diagnosis is made in adolescents (<10 years) or in adults, and usually the clinical form is mild. In the last rare cases of variants, named X91$^+$-CGD, mutated NOX2 is normally expressed (and membrane cytb_{558} too), but no NADPH oxidase activity can be detected. To date about 25 X91$^+$-CGD mutations have been reported [{Roos, 2010 #86}]. Most of them are missense mutations or small deletions, and are primarily located in the C-terminal cytosolic tail of NOX2, confirming the importance of this region in catalytic activity, but not in structural stability. This feature can be used to obtain insight in the importance of certain regions, but due to the scarcity of patient material, model systems are usually employed for detailed studies. Indeed 18 X91$^+$-CGD mutations have been reproduced in the PLB-985 cell line by mutagenesis, stable transfection and clonal selection, for functional studies [{Zhen, 1993 #37;Yu, 1999 #48;Zhen, 1998 #30;Li, 2005 #9;Li, 2007 #8;Debeurme, 2010 #106;Picciocchi, 2011 #105}].

We investigated 16 male patients suspected of suffering from X-linked CGD and their families. Clinical, genotypic, and phenotypic data are reported. These X-CGD patients were classified as having different variant forms of CGD (X91^0, X91$^-$ or X91$^+$) according to their NOX2 expression and NADPH oxidase activity. Twelve mutations in *CYBB* were novel. Two rare novel mutations (-67delT and a c.253-1879A>G mutation activating a splicing donor site) leading to X91$^-$-CGD were fully characterized. The impact of an intriguing double missense mutation Thr208Arg-Thr503Ile was also deciphered after stable transfection of Thr208Arg-NOX2 and Thr503Ile-NOX2 in the NOX2 knock-out PLB-985 cell line. The functional importance of novel missense mutations is discussed in the context of a new 3D model of dehydrogenase domain of NOX2 {Beaumel, 2017 #405}.

Materials and methods

Ethical considerations

Blood samples were collected from healthy volunteers, patients and relatives after obtaining their signed informed consent. Written consent for DNA analysis of samples from patients, parents and relatives was also obtained.

Patients

Patients from France, Croatia, Lithuania, and Finland were diagnosed as having CGD on the basis of their clinical history, examination and the inability of their phagocytes to generate reactive oxygen species (Tables 1 and 2). The results of the mosaic pattern by nitroblue-tetrazolium (NBT) assay or dihydrorhodamine-1,2,3 (DHR) flow cytometry from the mothers' peripheral neutrophils were consistent with an X-linked inheritance of the disease of their sons. X-CGD subtypes were determined according to the nomenclature $X91^0$, $X91^-$, $X91^+$ where the superscript denotes whether the level of NOX2 is undetectable (0), low ($-$) or normal (+) as determined by immunoblot or flow cytometry analysis. A summary of the clinical history of the patients is given in Table I. All patients are currently in good health under prophylactic treatment and are under constant care and follow-up in a specialized medical centre.

Cell preparation

Human neutrophils and mononuclear cells (lymphocytes plus monocytes) were isolated from citrated blood from patients, their relatives, and healthy volunteers. Lymphocytes purified by Ficoll-Hypaque density gradient centrifugation were infected with the B95-8 strain of EBV and cultured, as previously described [{Boyum, 1968 #355;Batot, 1998 #59}].

Wild-type (WT), X-CGD (lacking NOX2 expression and/or NADPH oxidase activity) and transfected X-CGD PLB-985 cell lines were grown in RPMI-1640 supplemented with 10% (v/v) fetal bovine serum, 100 units/ml penicillin, 100 µg/ml streptomycin, 2 mM L-Glutamine at 37 °C in a humidified 5% CO_2 atmosphere. Geneticin (0.5 mg/mL) was added to maintain the selection pressure of the plasmid in the transfected cells. For granulocytic differentiation, PLB-985 cells were exposed to 0.5% (v/v) dimethylformamide for 6 days [{Tucker, 1987 #102}].

ROS measurements in phagocytic cells

Reactive oxygen species (ROS) production in human neutrophils was measured by SOD-sensitive cytochrome c reduction, resorufine fluorescence measurement (Amplex Red® hydrogen peroxide⁄peroxidase assay kit, Invitrogen Life technologies, Villebon sur Yvette, France), flow cytometry with dihydrorodamine-1,2,3 (DHR) (TebuBio, Le Perray-en-Yvelines, France) or NBT slide test after opsonized latex bead phagocytosis, as previously described [{Martel, 2012 #131}]. In flow cytometry experiments with DHR, 5 µg/mL of catalase were added to the mother's neutrophils to avoid passive diffusion of ROS from oxidase-positive cells to oxidase-negative cells.

ROS production in PLB-985 cell lines was measured by chemiluminescence in the presence of luminol and horseradish peroxidase (HRPO) [{Li, 2005 #9}]. Relative light units (RLU) were recorded at 37°C, over a time course of 60 min in a Luminoscan luminometer (Labsystems, Helsinki, Finland).

In some experiment cells were labelled with 2.5 µg/mL Alexa Fluor 647 rat anti-human CD294 (CRTH2, BD Biosciences) as described below, prior of the incubation with DHR and PMA stimulation [{Defendi, 2009 #5}].

NADPH oxidase sub-units and CD294 expression in phagocytic cells

Flow cytometry – Single staining

FITC conjugated monoclonal antibody (mab) 7D5 directed against external epitopes of NOX2 (D162-3, Clinisciences, Nanterre, France), monoclonal anti-p22^{phox} (SC-130550, Santa Cruz Biotechnologies Inc, Heidelberg, Germany), with secondary antibody conjugated with Alexa Fluor 488 (A11070, Invitrogen Life technologies, Villebon sur Yvette, France) or PE (A10543, Invitrogen Life technologies, Villebon sur Yvette, France), were used for analysis of NADPH oxidase subunits expression in phagocytic cells. Control staining with appropriate isotype-matched control antibodies was included to establish thresholds for positive staining. Cell fluorescence was quantified using a FACS Canto II (BD Biosciences). Data were collected and analysed with the FACS DIVA software and FlowJo software-Tree Star (BD Biosciences, Pont de Claix, France).

Expression of NOX2 and CD294 in neutrophils and eosinophils by flow cytometry

Granulocytes (10^6 cells) were suspended in 0.1 mL of HBS-BSA and incubated with 5 µg/mL of mab 7D5 (anti-gp91^{phox}) or control isotype-matched IgG1 mab (02-6100, ThermoFisher Scientific, Illkirsh, France) for 30 min on ice. The cells were washed twice and incubated with Alexa-Fluor-488 goat-F(ab)$_2$ anti-mouse IgG1 (A11070, Invitrogen, Villebon sur Yvette, France) for 30 min on ice. After two washes as above, the cells were incubated with 2.5 µg/mL Alexa Fluor 647 rat anti-human CD294 (CRTH2, BD Biosciences, Pont de Claix, France for 30 min on ice and washed [[{Defendi, 2009 #5}].]. Cell-associated fluorescence (FL1 and FL4) was measured on 100,000 events. Data were collected and analyzed with the FACS DIVA software and FlowJo software-Tree Star (BD Biosciences, Pont de Claix, France).

Western blot

Expression of NOX2, p22^{phox}, p47^{phox}, p67^{phox} and p40^{phox} in a 1% Triton X100 soluble extract prepared from human neutrophils was examined by Western blot analysis using monoclonal antibodies anti-NOX2 48 and anti-p22^{phox} 449 {Verhoeven, 1989 #397}, polyclonal antibodies anti-p67^{phox} (C19, SC7662, Santa Cruz), anti-p47^{phox} and anti-p40^{phox} [{Vergnaud, 2000 #399;Stasia, 2013 #382}]. Polyclonal goat or rabbit anti-mouse IgG-HRP was used as a second antibody and the immune complexes were detected by chemiluminescence using an ECL kit Femtomax (Rockland Immunochemicals, Limerick, PA, USA). Protein concentration was determined by the Bradford method using Bio-Rad protein-assay reagent and bovine serum albumin as a standard [{Bradford, 1976 #47}].

Molecular analysis

Preparation of RNA and DNA

Total RNA was isolated from either mononuclear cells or EBV transformed B lymphocytes of both CGD patients and healthy individuals, using a modified single-step method [{Chomczynski, 1987 #144}]. Genomic DNA was purified with a purification kit (ref 51206 Flexigene DNA kit, Qiagen, Hilden, Germany).

Sequencing

When possible, first-strand cDNA was synthesized from total RNA by reverse transcriptase reaction according to the manufacturer's instructions (ref 11EMAMV203, MP Biomedicals Santa Ana, CA, USA). Total cDNA was immediately amplified by PCR in three overlapping PCR fragments and separated by gel electrophoresis [{Bakri, 2009 #387}]. The bands were photographed under UV (GelDoc XR+Biorad, Marnes-la-Coquette, France). All PCR products were sequenced using an ABI 3730 XL 96 capillary sequencer (Perkin Elmer, Foster City, CA, USA). All PCR products were sequenced using an ABI 3730 XL 96 capillary sequencer (Perkin Elmer, Foster City, CA, USA). More than 500 sequences of control cDNA of NOX2 were analyzed to rule out the possibility of polymorphisms.

In all cases, location of mutations found in cDNA was verified in *CYBB* genomic DNA after PCR amplification of each exon and flanking intron regions using appropriate forward and backward primers [{Bakri, 2009 #387}], followed by Sanger sequencing. This was done for all patients except for P1, P4a and P12. For patient P1 we used primers to amplify the promoter region of *CYBB* as previously described ({Defendi, 2009 #5}). For patients P4a and P12 new primers were designed to amplify a partial sequence of intron 3 (I3F-GAG AGT CTG AGT CAT TGC TCA G; I3R-CTA TCC GGA AGG TGG TCA TAG) and introns 8 and 9 (I8F-GCG ACA GAG GCA TTA TTT GGT T; I9R-CCT ATG TCT TGC CAG GAC ATC) of *CYBB*, respectively. Aliquot of all PCR products in bromophenol blue solution were run together with a DNA ladder (ref R0211, ThermoFisher scientific, Illkirch, France) on 1.5% (wt/vol) agarose containing Gel Red™ nucleic acid stain (ref 41003, Biotium, Inc, Fremont, CA, USA) in parallel with a negative control (PCR products amplified without DNA) and a positive control (PCR amplification of control DNA) to analyze size and purity. In some cases PCR products were purified from agarose gel according to manufacturer instruction (QIAquick Gel Extraction kit, ref 28704, Qiagen, Courtaboeuf, France).

Directed mutagenesis and stable transfection into X91-CGD PLB-985 cells

Thr208Arg and Thr503Ile point mutations were introduced into the wild-type (WT) NOX2 cDNA in pBluescript II KS(+) vector using the QuikChange site-directed mutagenesis kit (Stratagene, San Diego, CA, USA) according to the manufacturer's instructions. The sequence of WT and the mutated NOX2 cDNA were verified by dideoxynucleotide sequencing. The WT or mutant NOX2 cDNAs were subcloned into the mammalian expression vector pEF-PGKneo and electroporated into X-CGD PLB-985 cells in which the *CYBB* gene was disrupted by gene targeting, resulting in the absence of Nox2 expression and NADPH oxidase activity, as previously described ({Li, 2005 #9}). Clones expressing WT or mutated NOX2 were selected by limiting dilution in 1.5 mg/mL geneticin.

Results

Sum up of clinical data

X91-CGD patients were diagnosed from the age of one month (P6) to 26 years (P4a and P4b), but 10 patients out of 16 were diagnosed before the age of 2. The most frequent feature was prolonged fever, skin abscesses, adenopathies and pulmonary infections (Table 1). Some patients suffered from an inflammatory syndrome in the gastrointestinal tract (P2, P3, P4a, and P8). Patients P3, P8, P9 and P16 suffered from liver abscesses. The criteria of severity were defined according to the presence of severe infections in deep organs (lung, liver, bone…) associated with sepsis, and the age of first symptoms. Tissues examination of some patients (P2, P3, and P8) showed granuloma in skin, liver or tonsils. Patients P1, P4a, P7 and P10 suffered from skin infections and gastroenteritis only without infections in deep organs. Patient P1 was diagnosed at the age of 2 when he suffered from mild infections in the skin. A splenomegaly was detected at the time of diagnosis. He is now in good health under prophylactic treatment. Patient P4a had no susceptibility to infections during childhood and adolescence. He suffered from pollen allergy and mild asthma but he received no regular medication (Table 1). At the age of 13 he had recurrent perianal abscesses and fistulas. Crohn disease was suspected. In 2012 he had mild *S. aureus* infection around his nose. He was diagnosed at 26 years of age at the time of the death of his ~~twin~~ younger brother P4b from sudden-onset *Aspergillus pneumonitis*. P4a has been symptom-free for years and he's now in good health under prophylactic treatment; he became a father in 2014. Patient P7 had only superficial adenopathies and infections but was febrile and suffered from cyanosis and hypothermia. Six patients out of 16 suffered from sepsis or prolonged fever (P2, P6, P9, P10, P12, and P15) and one had a permanent hyperthermia (P2). *S. aureus* was the most frequently encountered bacterium (P2, P4a, P7, P10 and P14), *S. marcescens* being also found two times (P2, P3). Other bacteria were detected often at the origin of infections in CGD patients, such as *S. typhimurium* and *K. pneumonia, which* were found only in patient P12, *Mycobacterium bovis* in patient P11 and *Streptococcus spp* in patients P5 and P12. Pulmonary aspergillosis was found in patients P4a and P12, and suppurative inguinal adenopathies with *C. albicans* in P12 and at *S. aureus* in P10. Regarding the oldest patients P4a, P12 and P14, two of them were diagnosed early (P12 and P14) while patient P4a was diagnosed at the age of 26. This late diagnosis correlates perfectly with the level of severity of the disease (Table 1). This will be discussed according to the CGD subtypes these patients suffer from.

With respect to the treatment of CGD patients, all had a prophylactic life-long treatment (trimethoprim/sulfamethoxazole/itraconazole). Permanent corticosteroid therapy at low-dose was given to patients P2 and P14 because of a permanent hyperthermia and inflammatory syndrome (P2), and permanent respiratory failure required permanent oxygen therapy (P14). Four patients (P5, P8 P9 and P16) had bone marrow precursor cell transplantation at the age of 16 months to four years. Three patients have complete chimerism (P5, P9 and P16). Patient P5 suffered from chronic joint GvH, P16 had an acute digestive GvH and patient P8 had persistent diarrhea six-month post-transplant. Patient P9 is currently in good health.

Phenotypic and genotypic characterization of X91-CGD patients

The NADPH oxidase activity of purified neutrophils from the 16 X91-CGD patients and their relatives was measured by several different methods (as described in Materials and methods) and appeared totally abolished except for patients P1 and P4a (Table 2). We underline that the NADPH oxidase activities measured by the NBT reduction test correlate perfectly with those obtained by flow cytometry with the DHR probe in all the patients'

neutrophils. In addition, for the mothers (M1-2, M4, M5, M8, M10-11, M16), the percentage of "oxidase positive" neutrophils correlates perfectly with the percentage of neutrophils presenting a normal expression of NOX2 measured by flow cytometry (Table 2, Fig. 2). We confirm the large variation in the mothers' phenotype due to different X inactivation patterns. Only one mother was not carrier of the disease of her son (M7) (Fig. 2) but we did not investigate the mothers of patients P13 and P14. The daughter of patient P14 was diagnosed as a carrier as well (Table 2). In some cases, the absence of NADPH oxidase activity found in patients was measured by SOD-sensitive cytochrome c reduction (P6, P12, and P15) or resorufin oxidation (P3, P6, P14), which measures external production of superoxide (O_2^{-}) or hydrogen peroxide (H_2O_2), respectively (Table 2, Fig. 3a). However, these methods are less useful to detect a carrier status of mothers because the two populations of cells (oxidase-positive and -negative populations) cannot be distinguished by these methods. We also investigated the carrier status of maternal aunts, great-aunts and grandmothers too by looking for the genetic mutation found in the index X91-CGD patients (Gm2, Gam5, Am6, and Am15). None was carrier. The carrier status of some sisters of X91-CGD patients (S8, B8, and B12) was not fully investigated (no genetic analysis) because they were healthy and under-age for genetic diagnosis (to sign informed consent).

Normal NOX2 and p22^{phox} expression was found in patient P15's neutrophils even in absence of NADPH oxidase activity. This is a typical profile of a X91^{+}-CGD sub-type. In addition, for patients P1 and P4a, a faint NADPH oxidase activity with a low NOX2 and p22^{phox} expression was found that is typical for X91^{-}-CGD subtypes (Table 2). These cases will be discussed according to their specific genetic mutation.

X91^0-CGD patients

Thirteen of 16 X-linked CGD patients suffered from X91^0-CGD (except patients P1, P4a (X91^{-}-CGD) and P15 (X91^{+}-CGD). Indeed, neither NADPH oxidase activity nor NOX2 and p22^{phox} expression were found in the neutrophils of these 13 X^0 CGD patients (Table 2, Fig. 2a and b, Fig. 3a, b and c). Among these 13 patients we found four missense mutations, three small deletions, two nonsense mutations, one small insertion, one large deletion, one duplication and one splice mutation. The new double missense mutation c.637 C>G (exon 6) and c.1522 C>T (exon 12) leading p.Thr208Arg and p.Thr503ILeu mutations in NOX2 respectively ((patient P6), are responsible for a X91^0-CGD phenotype (Fig. 3a, b and c). This case is extremely rare in CGD. We previously published a similar double missense mutation p.His303Asn/Pro304Arg leading to a X91^{+}-CGD sub-type ({Stasia, 2002 #401;Bionda, 2004 #400}). Each of these last missense mutations was deleterious for the NADPH oxidase activity but not for its expression. In order to discard a possible polymorphism, we studied the functional impact of each mutation in the NOX2 knock-out PLB-985 cell line, as we previously did. Using directed mutagenesis and stable transfection in this cellular model, we found that each mutation (p.Thr208Arg and p.Thr503ILe) was deleterious for the NADPH oxidase activity (Fig. 3c), whereas only p.Thr208Arg mutation leads to the absence of NOX2 expression (Fig. 3d). However, we can conclude that neither mutation is a polymorphism. His mother is heterozygous for each mutation. The structural impact of each mutation together with those of the new missense mutation Val327Glu, will be discussed in the context of a 3D dehydrogenase model of NOX2 (Fig. 1 and Fig. 7) ({Beaumel, 2017 #405}).

X91⁺-CGD patients

Among 681 X-linked CGD cases reported in 2010 ({Roos, 2010 #86}) only 38 patients with 28 different mutations were identified as having an X91⁺-CGD sub-type. Often, these CGD variants are due to missense mutations ({O'Neill, 2015 #326}). The phenotype of Patient P15's neutrophils fit perfectly with this type of variant (Table 2). Indeed, all the NADPH oxidase sub-units were normally expressed in P15's neutrophils (Fig. 2c), whereas the NADPH oxidase activity was totally abolished (Table 2). A point mutation in exon 10 of *CYBB* (c.1235G>A) was responsible for the change of glycine-412 to glutamic acid in NOX2 (p.Gly412Glu) (patient P15) (Fig. 1). The total absence of NADPH oxidase activity correlates with the severe clinical profile found of this patient (Table 1). This mutation was reported in Roos et al., 2010, but not fully characterized ({Roos, 2010 #86}). Gly412 is in the dehydrogenase domain of NOX2 close to the NADPH binding site (Fig. 1). This will be discussed in the context of a 3D dehydrogenase model of NOX2 (Fig. 7) ({Beaumel, 2017 #405}).

X91⁻-CGD patients

A faint but significant NADPH oxidase activity was detected in the neutrophils of patients P1 and P4a (Table 2). The pattern of NOX2 expression was different in both patients. In patient P1, 97% of the neutrophils exhibited no NADPH oxidase activity, whereas about 3% of cells had a normal oxidase activity related to a normal expression of NOX2 (Table 2, Fig. 4a). This small population of cells was identified as eosinophils thanks to a CD294 double staining. However, a CD294 positive and oxidase negative population of cells was also highlighted (Fig. 4a). CD294, also known as CRTH2, is a seven-transmembrane G-protein-coupled receptor known as the chemoattractant receptor-homologous molecule expressed also in Th2 cells. Thus, maybe these cells were lymphocytes. The level of NOX2 expression is also in accordance with the percentage of both populations of cells (neutrophils and eosinophils) (Fig. 4b). NOX2 expression and the cytochrome b_{558} spectrum of patient P1's cells are due to eosinophilic contamination of the neutrophils after Ficoll purification (Fig. 4c). Using the same amount of proteins for each sample (control, mother and patient P1) (20 µg) loaded on the SDS-PAGE, a faint NOX2 and p22^{phox} expression in patient P1's granulocytes was seen by western blot analysis (Fig.4d). We verified that NOX2 was correctly glycosylated by performing a western blot with 200 µg of protein for patient P1 (data not shown). A novel -67delT mutation was found in the promoter region of *CYBB* (Fig. 4e). This point mutation is located in a region between the CCAAT and the TATA boxes in a consensus binding region of transcription factors (TFs) of the ets family (Elf1 and PU.1)({Eklund, 1996 #408};{Suzuki, 1998 #407};{Voo, 1999 #352}) (Fig. 4f). Others and we previously demonstrated that mutations located in this region disturb the binding of these TFs, which are necessary to trigger NOX2 expression ({Newburger, 1994 #349};{Weening, 2000 #350};{Defendi, 2009 #5}). However, in eosinophils, NOX2 expression is not under the control of these TFs ({Yang, 2000 #406}). This explains the NOX2 expression and the NADPH oxidase activity seen in the eosinophils of patient P1 (Fig. 6a and b).

For patient P4a, we found that the whole population of neutrophils exhibited a faint NADPH oxidase activity (Fig. 5a). This result correlates with the faint formazan staining of patient P4a's neutrophils in the NBT reduction test (Fig. 5b). A low NOX2 expression was also found in patient P4a's neutrophils by flow cytometry and western blot analysis, which correlates with the level of NADPH oxidase activity found in these cells (Fig. 5c and d). In addition, a substantial p22^{phox} expression was found in patient P4a's neutrophils, but in fewer amounts than in control neutrophils (Fig. 5e). His mother and his sister seemed to be carriers because they both possessed two populations of neutrophils, one oxidase-positive and an oxidase-negative population. This distribution was also seen in the NBT reduction test (Fig. 5b). However, the percentage of each population

differs in the mother and the sister of patient P4a (Fig. 5a). His mother has a major population of neutrophils with a normal oxidase activity (80% of the neutrophils) and the remaining neutrophils have a slight oxidase activity as seen in her son (20% of neutrophils), even in presence of catalase. In contrast, his sister has about 50% of neutrophils with a normal oxidase activity and 50% of cells with no oxidase activity (Table 2, Fig. 5a). This distribution is confirmed by the NOX2 and p22^{phox} expression profiles in their neutrophils (Fig. 5d and e). These differences are probably caused by different X inactivation patterns in both carriers.

To find the mutation in *CYBB* of patient P4a, NOX2 cDNA was amplified in 3 overlapping fragments from total mRNA by RT-PCR (Fig. 6a). Two bands were found in the first amplified fragment (β1-β2), one having a normal size (621 bp) corresponding to exon 1 to exon 6, the other having an abnormal higher size. Each band was excised, and cDNA was purified and sequenced. No mutation was found in the normal-sized band (exon 1 to exon 6). The sequence of the upper band showed an insertion of 124 bp of intron 3 as described in Table 2 and Fig. 6a. No mutations were found in the two other amplified fragments of cDNA (β3-β4 and β5-β6) (Fig. 6a). We sequenced all exons of *CYBB* with intronic flanking regions after PCR amplification from the genomic DNA of patient P4a and his relatives and no mutation was found. Then intronic regions surrounding the inserted region of intron 3 was amplified and sequenced. A novel c.253-1879A>G hemizygous mutation was found that activates a splicing donor site (Fig. 6b). The inclusion of the 124-bp fragment into the mRNA unveils an active cryptic acceptor site at the start of a pseudo-exon, and this inclusion is responsible for the partial loss of the NOX2 expression (Fig. 6b). Bioinformatic analysis allows the estimation of the splice donor sequence strength. The c.253-1879A>G mutation induces increase of the splice donor strength from 6.02 to 9.14 with the MaxEntScan matrix and from 83.52 to 95.58 with the HSF matrix (http://www.umd.be/HSF/technicaltips.html). The inserted sequence in the NOX2 cDNA creates a frameshift and introduction of a stop codon at position 85, explaining the loss of NOX2 expression (Fig. 6c). However, the neutrophils of patient P4a exhibited a low NOX2 expression related to a low NADPH oxidase activity by flow cytometry; it seems that a faint amount of normal NOX2 was expressed in his cells. The c.253-1879A>G mutation was also found in the genomic DNA of his mother and his sister in one allele, confirming their carrier status.

In conclusion, patients P1 and P4a suffer from an X91$^-$-CGD but the genetic mutation is very different for both patients, which can explain phenotypic differences between them. According to their clinical data, both patients suffer from a mild form of CGD.

Discussion

We reported here 16 patients with X-linked CGD (X91-CGD, OMIM #306400) presenting mutations in the *CYBB* gene. Most of the patients were from France except patients P4a, P11 and P13 who came from Finland, Lithuania and Croatia respectively. Most of the patients suffered from an X91^0-CGD, except patient P15 who had an X91$^+$-CGD and patients P1 and P4a who exhibited an X91$^-$-CGD. This classification is based on the level of NOX2 expression as previously demonstrated (Table 2). All types of mutations were found leading to X91^0-CGD type and 6 out of 13 were new and spread over the whole coding region (Fig.1 and Table 2). Regarding their clinical signs (Table 1), the X91^0-CGD cases were as far the most severe forms probably because of the absence of NOX2 expression and NADPH oxidase activity. Two out of these 6 new X91^0-CGD mutations were a point mutation in intron 6 (patient P7) and a large deletion (intron9/exon 9) (patient P12) leading to the deletion of exons 5/6 and exon 9, respectively (Table 2). In addition we analyzed an extremely

rare case of X91^0-CGD due to a double missense mutation (p.Thr208Arg and p.Thr503ILeu). To our knowledge it is the first listed case of a double missense mutation causing a X91^0-CGD. We previously published a unique case of a similar double missense mutation p.His303Asn/Pro304Arg leading to a X91$^+$-CGD sub-type ({Stasia, 2002 #401;Bionda, 2004 #400}). In this case, each missense mutation was deleterious for the NADPH oxidase activity but not for its expression ruling out the possibility of a polymorphism. However, polymorphisms are rare in *CYBB* ({Roos, 2010 #86}). In the present case, and regarding their respective position in the NOX2 model, each mutation acts through different mechanisms. Thr208 is located in the transmembrane segment V just upstream of His209, which is one of the proximal heme ligands. Thus, the mutation of this Thr208 in the heart of the membrane to an Arg, cumulating higher steric properties and a positive charge, may be deleterious to the structure of the transmembrane domain and at least locally may impair proper orientation of His209. This may lead in cascade to the absence of proximal heme and thus the impossibility to mature the final protein explaining a X91^0 phenotype for this modelized single mutant. Regarding Thr503ILe, the second cumulative missense mutation in this patient, its modelling in PLB985 leads to a normal expression but the loss of activity and thus a X91$^+$ phenotype. This Thr503 is located in a hot spot for X91$^+$-CGD mutations in the NIS (NOX Insertion sequence), which is a sequence specific of NOX dehydrogenase domains but absent in other structurally related dehydrogenase domain (e.g. ferredoxin NADP+ reductase) (see Fig. 7a). Previous mutations reported in the NIS have been shown to impair assembly with cytosolic factor and/or activation or the initial electrons transfer from NADPH to FAD ({Li, 2005 #9}; {Li, 2007 #8}; {Debeurme, 2010 #106}). Regarding to its location, the Thr503ILe mutation is likely to induce similar defect to those already studied and characterized in this NIS. {Beaumel, 2017 #405}. Among missense mutations in *CYBB* (Fig. 1), the p.Val327Asp mutation leading to a X91^0-CGD in NOX2 was new. This Val residue is located in the FAD binding subdomain of the NOX2 dehydrogenase domain (Fig.7a and b) and is at the center of a hydrophobic cluster within the domain. Introducing an aspartic acid in that position (Fig. 7b) is expected to disorganize the structure of the domain. This is fully compatible with the X91^0 phenotype within patient P10. Similar analysis can be drawn for the Trp516Arg mutant, where the Trp516 side chain is at the center of a hydrophobic cluster within the NADPH binding subdomain (Fig.7d). Its replacement by an Arg residue do not allow the correct folding.

Replacement of Gly412 by a glutamic acid lead to a X91$^+$ phenotype. At this position in the structure a glycine residue is strictly conserved, as well in the neighboring loops containing G408 and G538 (Fig7b). Addition of a Glu in this position may distort the proper packing of the Rossman fold and thus an efficient NADPH binding site. In addition, a Glu in this position adds a negative charge in the heart of the NADPH binding site which is already a strongly negatively charged coenzyme. These various elements explain a defective recognition of NADPH in such Gly412Glu mutant. {Beaumel, 2017 #405}. However, the clinical feature of this X91$^+$-CGD was as severe as X91^0-CGD cases because of the total absence of NADPH oxidase activity in phagocytes.

The clinical severity of X91$^-$-CGD is variable and depends on the localization of the mutations in *CYBB* arelated to the level of NADPH oxidase activity found in patients' phagocytes ({Beaumel, 2014 #337}; {O'Neill, 2015 #326}; {Kuhns, 2010 #316}). This X91$^-$-CGD variant is often due to missense mutations, small deletions or insertions in the encoding region of NOX2 (52 cases of X91$^-$-CGD listed in {Roos, 2010 #86}) leading to a decrease of its expression in phagocytes, the NADPH oxidase activity being slightly or totally abolished. We previously demonstrated that there are two categories of X91$^-$-CGD mutations, one in which the NADPH

oxidase activity is proportional to the NOX2 expression level and another one showing an absence of NOX activity associated with variable levels of NOX2 expression, the last one being associated with more severe clinical cases ({Beaumel, 2014 #337}). This work also permitted to point out potential binding regions of NOX2 with p22^{phox}, essential for normal synthesis of cytochrome b_{558}. In this work, the impact of the point mutation in intron 3 of *CYBB* on NOX2 expression and NADPH oxidase activity in phagocytes of patient P4a, was quite unusual. Indeed, a unique population of neutrophils was found by flow cytometry characterized by a faint NOX2 expression associated with a low NADPH oxidase activity, suggesting that normal mRNA was present in phagocytes (Fig. 6a and d). Indeed, even if mutated mRNA can be removed by Nonsense-Mediated mRNA Decay, the normal splice manages to remain in the patient P4a's neutrophils.   In addition, p22^{phox} expression was faintly impacted by this mutation (Fig. 6e). Thus, the clinical form of this X91$^-$-CGD case was mild. The faint but substantial NADPH oxidase activity found in the neutrophils 'population of patient P4a could partially protect him against infections. However, we must also underline that patient P4a had a younger brother P4b who died at 24 years of age of sudden onset *Aspergillus* pneumonitis. CGD was suspected only post mortem for patient P4b and ~~but~~ no biological investigation was done for him. Patient P4a was diagnosed after his brother´s death. He is now in good health and he is now a father for two children. Patient P1 suffered from a mild clinical form as it was the case for the other patients with this type of mutation ({Newburger, 1994 #349};{Weening, 2000 #350};{Defendi, 2009 #5}). Only five different mutations in the *CYBB* promoter leading to X91$^-$-CGD were documented in the literature (for review see {Stasia, 2008 #412}). Location of these mutations is situated in a region between the CCAAT and the TATA boxes in a consensus-binding region of transcription factors of the ets family (Elf1 and PU.1) that regulate NOX2 expression in neutrophils and monocytes ({Eklund, 1996 #408};{Voo, 1999 #352};{Suzuki, 1998 #407}). However, NOX2 expression is regulated differently in eosinophils ({Yang, 2000 #406}) explaining that patient P1 can partially be protected again infections because of the normal NADPH oxidase activity in his eosinophils.

In conclusion, in addition to rapid and efficient diagnosis provided by the new generation of high-throughput sequencing, certain rare monogenic disease like CGD, requires complete functional and molecular investigation to better understand the impact of each genetic mutation on the clinical severity of the disease. This refined characterization permit to understand the molecular mechanisms of the disease but also could give a help to the care and follow-up of patients with these rare diseases. In addition, the impact of missense mutations on the NADPH oxidase activity of CGD patients, can be explained thanks to the 3D model of the dehydrogenase domain of NOX2 which enables to improve our knowledge of the functioning of this enzyme.

Table 1
Clinical data of X91-CGD patients

Patients	X91-CGD variants	Date of birth	Age of diagnosis	Severe clinical signs	Minor clinical signs	Actual treatments[a]
P1	X91[-]	12/22/13	01/20/15	/	Multiple abscessed skin lesions, Splenomegaly	Prophylactic[b]
P2	X91[0]	11/18/12	09/24/14	Permanent hyperthermia	Inflammatory syndrome, xanthogranuloma (*S. marcescens*), tonsil adenophlegmon (*S. aureus*), microcytic anemia due to martial deficiency, diarrhea, vomiting, rotavirus gastroenteritis	Prophylactic[b]
P3	X91[0]	03/10/09	01/01/2012	Sepsis, hepato-splenomegaly hepatic granuloma	Pallor, pustulosis, inflammatory syndrome, bloody diarrhea (*Enterococcus faecium*), multiple necrotic adenopathies (*S. marcescens*), hepatic cytolysis and cholestasis, failure to thrive	Prophylactic[b]
P4a[c]	X91[-]	02/04/86	18/10/2012	/	Mild childhood asthma, at teen-age recurrent perianal abscesses, treated for Crohn disease, nose infection (*S. aureus*)	Prophylactic[b]
P4b[c†]		1988	2012 post mortem	*Aspergillus* pneumonitis	/	/
P5	X91[0]	07/29/12	07/29/12	Pulmonary abscesses (*St.constellatus*)	Neonatal pustular melanosis, eosinophilic pancolitis, maculo-papular skin rash	Engrafment at 3 years of age. Chronic joint GvH. Complete chimerism
P6	X91[0]	03/13/09	04/28/09	Severe sepsis, three outbreaks of pneumonia	/	Prophylactic[b]
P7	X91[0]	06/20/16	06/22/17	/	Cervical adenitis, febrile (*S. aureus*), papular lesions, fungal infections in the penis, hypothermia, cyanosis	Prophylactic[b]
P8	X91[0]	12/08/15	05/19/16	Hepatic abcesses	Fever, inflammatory syndrome, rotavirus gastroenteritis, cervical adenopathies, granuloma of the tonsil, perforated acute otitis, Ileitis	Recent engrafment (HLA id.) with infectious complications and viral reactivation, persistent diarrhea six months post-transplant

P9	X91^0	10/28/12	06/02/14	Prolonged fever, liver abscesses	/	Engrafment at 3 years of age, complete chimerism. In good health
P10	X91^0	09/02/18	12/18/18	Bacteriemia (*St. Aureus*)	Reccurent suppurative inguinal (*St. Aureus*)	Prophylactic[b]
P11	X91^0	14/10/14	03/15/17	*Mycobacterium bovis* infection	Recurrent suppurative lymphadenitis, pneumonia, other pulmonary bacterial infections/	Prophylactic[b]
P12	X91^0	01/30/86	06/24/87	Sepsis (*S. typhimurium*), pulmonary aspergillosis	Suppurative inguinal adenopathies (*C. albicans*), furonculosis (*K. pneumoniae*), cervical adenopathy (*Streptoccocus*), balano-prepucial fistula, recurrent cold sores	Prophylactic[b]
P13	X91^0	09/07/13	07/20/16	Abscess of the mediastinum, bacteremia, bacterial pneumonia, suspected Noonan syndrome	Cervical lymphadenitis, BCGitis	Prophylactic[b]
P14	X91^0	09/21/10	12/02/10	Bone infection (*St. Aureus*) treated by laminectomy, permanent respiratory failure (restrictive and obstructive)	Peritonsillar abcess	Prophylactic[b], corticotherapy, hydroxychloroquine, amethopterine, permanent oxygenotherapy
P15	X91$^+$	12/19/03	09/20/09	Prolonged fever, pulmonary abcess	Cervical adenopathy, BCGititis, abscess of the anal margin, acute appendicitis, diarrhea recurrent fevers, chronic inflammation syndrome	Prophylactic[b]
P16	X91^0	01/21/13	06/30/16	Liver abcesses	Cervical adenitis	Engraftment at 16 months years of age, acute digestive GvH, Bronchiolitis Obliterans Syndrome, complete chimerism

[a]possibly engrafment
[b]Trimethoprim-sulfamethoxazole and itraconazole
[c]P4a and P4b are sibling X91-CGD patients, P4b died at 24 years old. At that time CGD diagnosis was done.
[†]Dead patient

Table 2
Phenotypic and genotypic profiles of X91-CGD patients

Patients	NBT test % of positive cells	Cyt c Red O_2^- nmol/min /10^{6}cells[a]	Resorufin H_2O_2 nmol/min /10^{6}cells[b]	DHR, Index (% of cells)[c]	Protein expression flow cytometry Index (% of cells) or WB	Cytb_{558} picolmol/ mg proteins	cDNA nucleotide change	Gene location	Amino-acid change	CGD-type
P1	/	/	/	2.3 (98)-277 (2)	1.0 (98)-25,1 (2)	/	-67 delT	Promoter	No	X⁻
M1		/	/	4.3 (36)-22.3 (63)	1.0 (33)-17,1 (67)					Carrier
P2		/	/	1.1 (100)	1.1 (100)		c.39delT	Exon 1	p.Phe13LeufsX21	X⁰
M2		/	/	2.6 (47)-47.0 (53)	1.0 (46)-18.9 (54)					Carrier
Gm2	/	/	/	/	/	/				Not carrier
P3	1.0	/	0 - 0 - 0	1.0 (100)	Abs NOX2	/	c.201dupT	Exon 3	p.Leu68SerfsX34	X⁰
P4a	21.0	/	/	10.4 (100)	2.3 (100)	36	c.253-1879A>G	Intron 3	Skip exon 3, p.Cys85LeufsX32	X⁻
M4	80	/	/	3.4 (16)-13.4 (84)	2.8 (10)-30.0 (90)	342				Carrier
S4	58	/	/	1.2 (47)-12.4 (53)	2.2 (37)-30.0 (63)	315				Carrier
P5	0	/	/	1.0 (100)	1.0 (100)		c.600_603dupTTAC	Exon 6	p.Phe202LeufsX2	X⁰
M5	30	/	/	8.4 (78)-49.8 (22)	1.0 (65)-55.0 (35)					Carrier
Am5	72	/	/	2.1 (24)-6.9 (76)	1.0 (17)-9.3 (83)	/				Carrier
Gam5	/	/	/	/	/	/				Not carrier
P6	0	0 - /	0 - 0 - 0			0	c.623 C>G and c.1508 C>T	Exon 6 and Exon 12	p.Thr208Arg and Thr503ILe	X⁰
M6	39	5.5 - /	1.4 - 10.4 - 5.5		/	76				Carrier
Am6	/	/	/	/	/	/				Not Carrier
P7	0			1.3 (100)	1.3 (100)		c.674+3G>T	Intron 6	Deletion of exon 6 or exon 5 and 6, p.Asp162ThrfsX15	X⁰
M7	94	/	/	57.8 (100)	44.7 (100)					Not carrier
P8	0	/	/	1.0 (100)	1.2 (100)		c.676C>T	Exon 7	p.Arg226X	X⁰
M8	49	/	/	39.0 (48)-154 (52)	1.2 (49)-19.0 (51)					Carrier
S8[d]	94	/	/	15.5 (100)	8.3 (100)	/	/			ND[d]
B8[d]	/	/	/	/	/	/	/			ND[d]
P9	0	/	/	1.0 (100)	1.0 (100)	/	c.816G>A	Exon 8	p.W272X	X⁰
M9	36	/	/	2.8 (78)-25.0 (22)	1.0 (60)-23.0 (40)					Carrier
Am9	90	/	/	158 (100)	12 (100)					Not carrier
Am9'	96	/	/	97 (100)	20 (100)					Not carrier
Gam9	/	/	/	63 (100)	10 (100)					Not carrier
P10	/	/	/	1.0 (100)	1.0 (100)	/	c.980T>A	Exon 9	Val327Asp	X⁰

M10	/	/	/	46.0 (58)-244 (42)	1.0 (64)-23.0 (46)					Carrier
P11	0	/	/	1.0 (100)	1.0 (100)	/	c.1061_1065delATATC	Exon 9	p.His354ProfsX16	X⁰
M11	12	/		3.5 (93)-217 (7)	1.3 (90)-44.7 (10)					Carrier
P12	0	0 - 0	/		Abs NOX2	0	c.897+1258_1151+129del (del of 1657bp)	Intron9/Exon 9	Skip exon 9, p.Val300AspfsX4	X⁰
M12	57	1.9 - 0.9	/	/	NOX2 diminished	39				Carrier
S12	73	5.0 - 1.4	/	/	NOX2 diminished	55				Carrier
B12[d]	80	10.0 - 5.6	/	/		103				ND[d]
P13	2	/	/	/	Abs NOX2	/	c. 1166G>A	Exon 10	p.Gly389Glu	X⁰
P14	4	/	0 - 0 - 0	/	Abs NOX2 *?*	/	c.1167_1179delGCCCTTTGGCACT	Exon 10	p.Phe391ValfsX9	X⁰
D14	48	/	/	/		/				Carrier
P15	0	0	/	/	Pres NOX2	/	c.1235G>A	Exon 10	p.Gly412Glu	X⁺
M15	88	14.6	/	/		/				Carrier
Am15	/	/	/	/	/	/				Not carrier
P16	4	/	/	1.1 (100)	1.2 (100)	/	c.1546T>C	Exon 12	p.Trp516Arg	X⁰
M16	36	/	/	42 (68)-189 (32)	2.0 (69)-35.9 (31)	/				Carrier

P, patient; M, mother; Gm, grand-mother; S, sister; B, brother; D, daugther; Am, maternal aunt; Gam, maternal grand-aunt.
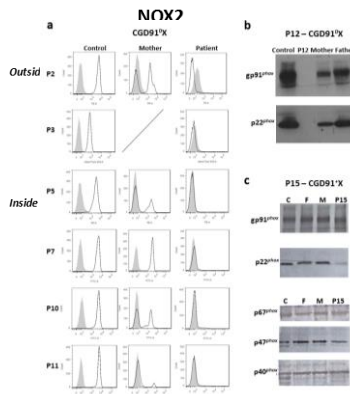
[a]Activation with PMA and opsonized zymosan

[b]Activation with PMA, Opsonized zymosan and PAF/fMLF

[c]MFI of activated cells/MFI resting cells (% of cells having index) or western blot 's results; Abs = Absence, Decr = Decrease

[d]Genetic analysis not done because they were safe and not of age.

In bold are new mutations in *CYBB*.

Fig. 1 Schematic representation of X-linked CGD mutations within the NOX2 protein – New mutations are in red and known mutations are in blue. New mutations in the promoter (Patient P1) or in intron sequences (Patients P4a and P12) of *CYBB* are not represented.

Fig. 2 Phenotypic analysis of the neutrophils from X-linked CGD patients having new *CYBB* mutations. NADPH oxidase activity of patients and their mothers' neutrophils was measured by flow cytometry after stimulation during 15 min with 20 ng/mL PMA in presence of dihydrorodamine (DHR) probe as described in Materials and methods. Solid grey curve correspond to DHR loaded resting neutrophils, empty black curve correspond to DHR loaded neutrophils after PMA stimulation (**a**). For patient P12, the absence of gp91^{phox} (or NOX2) and p22^{phox} expression was shown by western blotting using the primary specific antibodie 48, 449 respectively (**b**). Note that all the sub-units of the NADPH oxidase complex are expressed in patient P15's neutrophils (X91$^+$-CGD) by western blotting using specific antibodies as described in Material and methods.
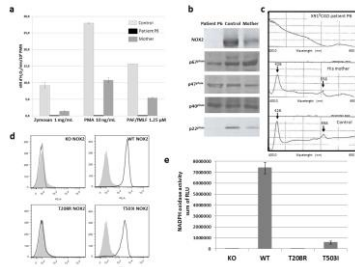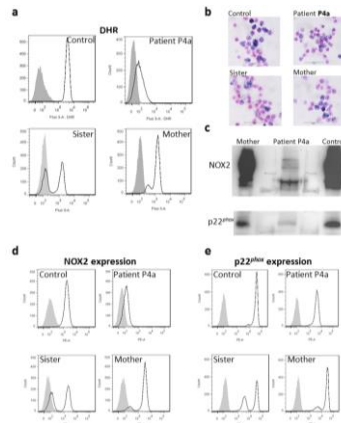
Fig. 3 Functional analysis of patient P6's T208R and T503I substitutions in NOX2 by means of transgenic PLB-985 cells. Measurement of the NADPH oxidase activity of neutrophils of patient P6 and of his mother by resorufine oxidation (Amplex Red^R) after opsonized zymosan, PMA and PAF/fMLF activation as described in Materials and methods (**a**). Expression of NADPH oxidase sub-units NOX2, p67^{phox} and p47 ^{phox} p40 ^{phox} and p22 ^{phox} in patient P6 and his mother's neutrophils by western blot analysis (**b**). Cytochrome b_{558} differential spectra of 1% Triton X100 soluble extract from patient P6 and his mother's neutrophils (**c**). NOX2 expression in differentiated T208R-NOX2 and T503I-NOX2 transgenic PLB-985 cells by flow cytometry using the FITC coupled 7D5 monoclonal antibody against NOX2. Solid grey curve correspond to resting neutrophils labelled with monoclonal Mouse IgG1 isotype as an irrelevant antibody, empty black curve correspond to neutrophils labelled with FITC coupled 7D5 (**d**). NADPH oxidase activity of differentiated T208R-NOX2 and T503I-NOX2 transgenic PLB-985 cells measured by chemiluminescence in presence of luminol, HRPO after 20 ng/mL PMA stimulation (**e**).
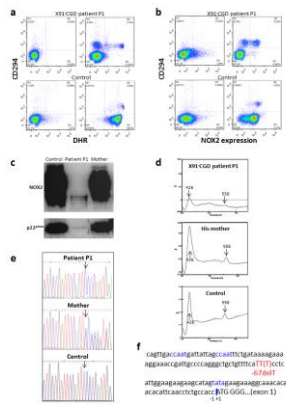
Fig. 4 Phenotypic and genotypic characterisation of the X91⁻-CGD of patient P1 due to a new point mutation in the *CYBB* promoter. Flow cytometry dot plots of NADPH oxidase activity (DHR) and CD294 expression (eosinophil marker) in neutrophils and eosinophils of granulocyte preparations from a healthy subject (bottom panels) and patient P1 (top panels) at rest (left panels) or after stimulation with PMA (right panels). Left panels correspond to dot plots of cells labelled with isotype control antibodies and loaded with DHR. (**a**). Flow cytometry dot plots of NOX2 and CD294 expression (eosinophil marker) in neutrophils and eosinophils of granulocyte preparations from a healthy subject (bottom panels) and patient P1 (top panels) using 7D5 monoclonal antibody and anti-CD294 antibody (right panels) compared to dot plots of isotype controls (left panels) (**b**). NOX2 and p22*phox* expression in patient P1 and his mother's granulocytes by western blot analysis. A faint NOX2 and p22*phox* expression are visible probably due to the presence of eosinophils in the granulocyte preparation (**c**). Cytochrome b_{558} differential spectra of 1% Triton X100 soluble extract from patient P1 and his mother's neutrophils (**d**). Thymidine deletion at position -67 detected in the *CYBB* promoter region of patient P1 and his mother as a carrier, compared to a healthy donor sequence (**e**). Schematic representation of part of the *CYBB* promoter region, with localization of the "CCAAT" and "TATA" boxes, the ATG starting codon and the point mutation described in panel e (**f**).

Fig.5 Phenotypic analysis of the from an from X91⁻-CGD patients and NADPH oxidase activity of patient s'neutrophils was measured by flow min with 20 ng/mL PMA in presence described in Materials and methods. loaded resting neutrophils, empty loaded neutrophils after PMA activity of patient P1, his sister and also measured using the NBT expression was shown by western antibodies 48 and 449 respectively (**e**) was shown by flow cytometry

neutrophils of patient P4a suffering having 1 new *CYBB* mutation. P1, his sister and and his mother cytometry after stimulation during 15 of dihydrorodamine (DHR) probe as Solid grey curve correspond to DHR black curve correspond to DHR stimulation (**a**). The NADPH oxidase and his mother s' neutrophils was reduction test (**b**). NOX2 and p22^{phox} blot using the primary specific (**c**). Nox2 (**d**) and p22^{phox} expression using the primary specific antibodies

7D5 and 449 respectively. Solid grey curve correspond to resting neutrophils labelled with irrelevant antibodies, empty black curve correspond to neutrophils labelled with FITC coupled 7D5 (NOX2) or 449 antibodies (p22^{phox}) and secondary antibodies coupled with PE.
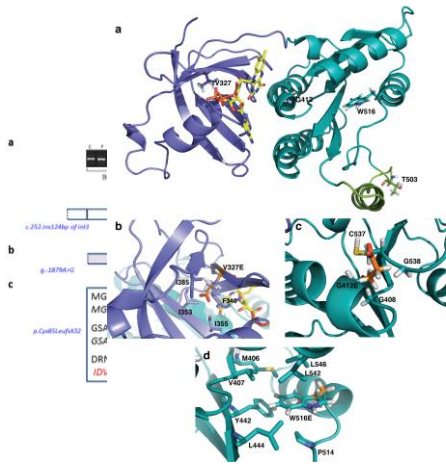
Fig. 6 Genetic analysis of the mutation of patient P4a in *CYBB* gene, leading to an X91⁻-CGD. NOX2 cDNA was amplified in 3 overlapping fragment as described in Materials and methods. A 124 bp of intron 3 was inserted between exon 3 and exon 4 leading to the creation of a pseudoexon (**a**). Intronic regions surrounding the inserted region of intron 3 in the NOX2cDNA was amplified and sequenced. A c.253-1879A>G hemizygous mutation was found creating a splicing donor site, which unveils a cryptic acceptor site leading the inclusion of 124 nucleotides as a pseudo-exon responsible for the partial loss of the NOX2 expression (**b**). The consequence in the NOX2 protein is a missense mutation at Cys85 to Leu and a frameshift leading to the generation of a stop codon located 32 amino acids further on (p.Cys85LeufsX32) (**c**).

Fig. 7. NOX2 dehydrogenase model and modelisation of CGD mutations. (**a**) The DH model is represented as ribbons, dark green for the NADPH binding domain -corresponding to the 3A1F pdb structure- and purple blue for the modelled FAD binding domain ({Beaumel, 2017 #405}). NOX2 NIS, in light green, is an approximate structural model but is partly disordered, flexible as suggested by the absence of density in the 3A1F structure for this sequence. Some of the residue corresponding to X91⁰ and X91⁺ mutations are highlighted as shown in stick (V327, G412, W516, T503). (**b**), (**c**) and (**d**) are zoom around V327, G412 and W516 with emphasis on the neighboring residues around the considered mutations. In each case, the mutated position is presented with both the wild type side chain and the corresponding mutation, in orange, superimposed. Molecular graphic images were produced using PyMOL software. W516R, V327D